

# **Isolation of RNA from a Mixture and its Detection by Utilizing a Microgel-Based Optical Device**

Molla R. Islam, Shakiba Azimi, Faranak Teimoory, Glen Loppnow\* and Michael J. Serpe\*

Department of Chemistry, University of Alberta

Edmonton, AB, Canada

\*Corresponding authors

E-mail: [serpe@ualberta.ca](mailto:serpe@ualberta.ca) and [gloppnow@ualberta.ca](mailto:gloppnow@ualberta.ca)

Keywords: Stimuli-responsive polymers; Optical sensors; Poly(*N*-Isopropylacrylamide)-based microgels; RNA sensing

## **Abstract**

In this investigation, we show that RNA can be separated from a solution containing DNA and RNA, and the isolated RNA detected using poly (*N*-isopropylacrylamide-*co*-*N*-(3-aminopropyl) methacrylamide hydrochloride) microgel-based optical devices (etalons). The isolation of RNA was accomplished by using hairpin-functionalized magnetic beads (MMPDNA) and differential melting, based on the fact that the DNA-RNA hybrid duplex is stronger (i.e., high melting temperature) than the DNA-DNA duplex (i.e., low melting temperature). By performing concurrent etalon sensing and fluorescent studies we found that the MMPDNA combined with differential melting was capable of selectively separating RNA from DNA. This selective separation and simple colorimetric detection of RNA from a mixture will help lead to future RNA-based disease diagnostic devices.

## Introduction

The structure of RNA in a given system is remarkably complex, diverse and unique, with their structures tied to their very specific functions. Their sizes are also different, from very short siRNA sequences to much longer mRNA. It is very important to isolate and study a specific RNA for sequencing, cloning and gene silencing with a goal to develop future point-of-care (POC) devices.<sup>1</sup> RNA-linked diseases include myotonic dystrophy and fragile X-associated tremor/ataxia syndrome.<sup>2</sup> Also, interference RNA is being used to treat diseases such as HIV, viral hepatitis, cardiovascular and cerebrovascular diseases, metabolic disease, neurodegenerative disorders and cancer.<sup>3</sup> There are number of available techniques for RNA detection and separation including western blot, PCR and qPCR each exhibiting their own sensitivity and selectivity.<sup>4</sup> All of these techniques require the use of expensive instruments operated by highly trained professionals to yield acceptable results and thus, their use for POC applications is limited.

The use of responsive polymeric materials (i.e., smart materials) in sensing technologies is extremely promising due to their ability to translate molecular information into a signal that can be captured for quantitative analysis.<sup>5</sup> Thermoresponsive poly(*N*-isopropylacrylamide) (pNIPAm) is the most widely studied responsive polymer due to its ability to respond to changes in temperature near physiologically relevant temperatures.<sup>6-9</sup> The thermoresponsivity is manifested as a conformational change of the polymer from a random coil (extended state) to a

globule (collapsed state) as the temperature of water that the polymer is dissolved in exceeds 32 °C.<sup>10,11</sup> The pNIPAm can also be crosslinked to form hydrogels and colloiddally stable hydrogel micro and nanoparticles (microgels and nanogels, respectively).<sup>12,13</sup> By taking advantage of the ease of synthesizing and chemically functionalizing microgels, multiresponsive microgels have been generated and utilized for various applications.<sup>6, 14, 15</sup>

Since 2009, the Serpe group has been working on optical devices composed of a single layer of pNIPAm-based microgels sandwiched between two Au layers, as shown schematically in Fig. 1a. This device exhibits visible color and multippeak reflectance spectra (Fig. 1b) upon exposure to white light. We have shown that at a given angle of observation, the position of the reflectance peaks depends primarily on the distance between the device's two Au layers. The position of the peaks in a reflectance spectrum can be predicted from Eq. (1):

$$m\lambda = 2nd \cos\theta \quad (1)$$

where  $n$  is the refractive index of the microgel (dielectric) layer,  $d$  is the mirror–mirror distance,  $\theta$  is the angle of incident light relative to the normal, and  $m$  (an integer), is the order of the reflected peak.

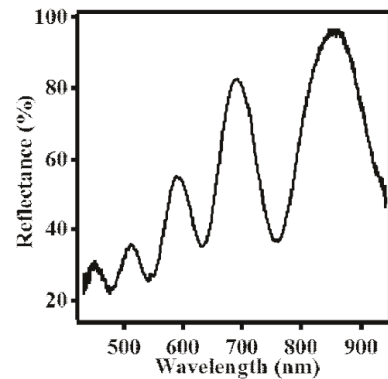
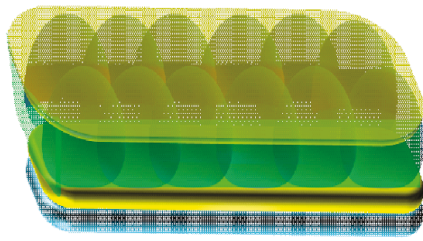


Fig. 1: (a) The structure of a typical microgel-based etalon and (b) a representative reflectance spectra.

By exploiting the solvation state changes the microgels can undergo in response to temperature (and other stimuli), we have shown that microgel-based materials and etalons can be used for sensing and biosensing, drug delivery and water remediation applications.<sup>16-19</sup> We extended the sensing capability of the etalon to sense single stranded target DNA from mixture of other non target single stranded DNA. We have also shown that the target DNA can be detected in the presence of single stranded DNA with 2 or 4 base mismatches.<sup>18</sup> In these studies, we found that the optical response (shift in the position of the peaks in the reflectance spectra) was directly related to the concentration of the target DNA. In this paper, we show that RNA with a specific sequence can be isolated from a solution also containing DNA, and the isolated RNA can be detected using etalons composed of positively charged pNIPAm-co-N-(3-aminopropyl)methacrylamide hydrochloride (pNIPAm-co-APMAH) microgels. The separation was based on the known fact that DNA-DNA duplexes are weaker

than DNA-RNA hybrid duplexes. We show that a target RNA sequence can be separated from a mixture of DNA and RNA using DNA hairpin-functionalized magnetic microparticles and exploiting their differential melting profiles. The DNA hairpin was designed such that it shows specificity and selectivity towards the target RNA. The selectivity and separation efficiency were confirmed by fluorescent labelling of the RNA and DNA. This approach represents a very simple and straightforward method to selectively separate and detect RNA with a specific sequence from a solution, which could find downstream biological/biomedical applications for real-time PCR, microarray analysis, next-generation sequencing (RNA-Seq), northern blotting, and cloning.

## **Experimental Details**

### **Materials**

N,N'-methylenebisacrylamide (BIS) (99%), ammonium persulfate (APS) (98.5%), and DMSO were obtained from Sigma-Aldrich (Oakville, ON) and were used as received. N-(3-Aminopropyl) methacrylamide hydrochloride (APMAH) was purchased from Polysciences, Inc. (Warrington, PA). *N*-Isopropylacrylamide (NIPAm) was purchased from TCI (Portland, Oregon) and purified by recrystallization from hexanes (ACS reagent grade, EMD, Gibbstown, NJ) prior to use. Sodium chloride was obtained from Fisher (Ottawa, ON) and used as received. Deionized water (DI) was obtained from a Milli-Q Plus system from Millipore (Billerica, MA) and was filtered to have a resistivity of 18.2 M $\Omega$ •cm. Chromium (99.999%) was obtained from ESPI (Ashland, OR), and gold (99.99%) was obtained from MRCS Canada (Edmonton, AB). Chromium and gold layers were deposited using a model THEUPG thermal evaporation system from Torr International Inc. (New Windsor, NY). The glass cover slips coated with Cr/Au were

annealed in a Thermolyne muffle furnace from Thermo Fisher Scientific (Ottawa, Ontario). Anhydrous ethanol was obtained from Commercial Alcohols (Brampton, Ontario). Fisher Scientific's (Ottawa, Ontario) Finest prewashed glass coverslips were used and were 25×25 mm. Succinimidyl 4-(p-maleimidophenyl)butyrate (SMPB) and dithiothreitol (DTT) were purchased from Pierce Biotechnology, Inc. (Rockford, IL). The 5'-thiol modified DNA hairpin oligomers, and DNA and RNA tagged with fluorescent labels were purchased from IDT (Coralville, IA, USA). Amine functionalized magnetic beads (Dynabeads M-270 amine) were purchased from Life Technologies Corporation (Frederick, MD, USA).

## **Procedures**

### **Poly(*N*-isopropylacrylamide-*co*-*N*-(3-Aminopropyl)methacrylamide hydrochloride) (pNIPAm-*co*-APMAH) Microgel Synthesis**

pNIPAm-*co*-APMAH microgels were synthesized via temperature-ramp, surfactant-free, free radical precipitation polymerization as described previously.<sup>20</sup> The reaction mixture was comprised of 90% *N*-isopropylacrylamide (NIPAm) and 5% *N*-(3-Aminopropyl)methacrylamide hydrochloride (APMAH) with 5% *N,N'*-methylenebisacrylamide (BIS) used as a crosslinker. The monomer, NIPAm (18.0 mmol), and BIS (1.0 mmol) were dissolved in DI water (100 mL) with stirring in a beaker. The mixture was filtered through a 0.2 μm filter affixed to a 20 mL syringe into a 200 mL 3-neck round-bottom flask. The beaker was rinsed with 25 mL of DI water and then filtered into the NIPAm/BIS solution. The flask was then equipped with a temperature probe connected to a temperature control system, a condenser, N<sub>2</sub> gas inlet (a needle), and a stir bar. The solution was purged with N<sub>2</sub> gas for about 1.5 h, with the stirring set to a rate of 450

rpm, while the temperature was allowed to reach 45 °C. APMAH (1.0 mmol) solution was then added with a micropipette in one aliquot. A 0.078 M aqueous solution of APS (5 mL) was delivered to the reaction flask with a transfer pipet to initiate the reaction. Immediately following the initiation, a temperature ramp of 45 to 65 °C was applied to the solution at a rate of 30 °C/h. The reaction was allowed to proceed overnight at 65 °C. After polymerization, the reaction mixture was allowed to cool down to room temperature and filtered through glass wool to remove any large aggregates. The aggregates were rinsed with DI water and filtered. Aliquots of these isolated microgels (13 mL) were centrifuged at a speed of ~8500 relative centrifugal force (rcf) at 23 °C for about 60 min to produce a pellet at the bottom of the centrifuge tube. The supernatant was removed from the pellet of microgels, which was then resuspended to the same volume (13 mL) of DI water. Centrifugation and re-suspension was repeated five more times to remove any unreacted reagents, linear polymers, and oligomers present with the microgel. After repeated centrifugation, a pure, concentrated, and very viscous microgel pellet was formed and kept in the centrifuge tube for further use.

### **Synthesis of DNA-Functionalized Magnetic Microparticles (MMPDNA)**

The preparation of DNA functionalized MMPs has been reported elsewhere.<sup>21</sup> In short, amino-functionalized magnetic microparticles (MMPs, 2.8- $\mu$ m diameter; Invitrogen) were covalently linked to 5'-thiol-modified oligonucleotides (IDT) with heterobifunctional crosslinker succinimidyl 4-[p-maleimidophenyl] butyrate (SMPB) (Pierce Biotechnology, Inc.). The oligonucleotide was designed with a poly-dA<sub>10</sub> universal linker and the base sequence was selected such that it forms a hairpin

(5'-/5ThioMC6-D/AAAAAAAAAAACCCAGTAACCTAACCTCGACACTGGG-3'). First, the MMPs (30 mg mL<sup>-1</sup>, 1 mL) were washed twice with 1 mL of anhydrous DMSO in a 1.5 mL microcentrifuge tube. A fresh solution of 10 μM SMPB (50 mg) in DMSO was prepared prior to the reaction (the sample vial was washed with DMSO and collected to avoid sample loss). The SMPB/DMSO solution was added to the magnetic beads, and the reaction between the primary amino group and the *N*-hydroxysuccinimide (NHS) ester of SMPB was allowed to proceed for 4 h with gentle shaking at room temperature. The reaction with SMPB was carried out in the dark. Then, the disulfide bonds in all 5'-thiolated oligonucleotides were reduced by DTT. 100 μL of a freshly prepared 0.1 M DTT solution in disulphide cleavage buffer (170 mM phosphate, pH 8.0) was added to 25 nmol lyophilized DNA in a microcentrifuge tube, wrapped in aluminum foil with occasional stirring for 2.5 h. After that time, DTT-DNA mixture was passed through NAP-5 column (GE Healthcare Life Sciences, London, UK) and collected into a series of microcentrifuge tubes by adding 1.35 mL of DI water. The location and concentration of DTT-reduced DNA was confirmed by UV-visible spectrophotometry and 350 μL of 10 μM solution was prepared with coupling buffer (0.2 M NaCl, 100 mM phosphate, pH 7.0) by appropriate dilution. This DNA solution was kept at 2-8 °C to be used to couple with SMPB functionalized magnetic beads. The reaction between SMPB and magnetic beads was stopped after 4 h. The beads were magnetically separated and washed three times with DMSO (10 mL) and two times with coupling buffer (0.2 M NaCl, 100 mM phosphate, pH 7.0; 10 mL). Now 300 μL of the 10 μM DTT-reduced DNA solution was added to the washed SMPB-activated magnetic beads. The rest of the DTT-cleaved DNA solution was kept for calculating the coupling efficiency. The reaction between the maleimide group and the SH group of the DNA

was allowed to proceed at room temperature for 2 h under constant stirring. Next, the DNA-functionalized beads were placed on a high pull magnet (Eclipse Magnetics, Sheffield, UK), the supernatant was removed and preserved, and the beads were washed three times with coupling buffer and then twice with passivation buffer (0.15 M NaCl, 150 mM phosphate, pH 8.0). The supernatant was used to determine the coupling efficiency by measuring the absorbance at 260 nm and comparing it with the absorbance of DTT-cleaved DNA prepared for DNA functionalization. The coupling efficiency of the DNA functionalized magnetic microparticles, MMPDNA was calculated to be 95%. The unreacted amine (if any) on the surface of the DNA-functionalized MMPs was passivated by adding a freshly prepared 10  $\mu$ M solution of sulfo-NHS-acetate (100 mg in ~ 40 mL passivation buffer). The passivation process was allowed to proceed for 1 h at room temperature with mild shaking. The beads were washed twice with passivation buffer, twice with storage buffer (10 mM phosphate, 200 mM NaCl; pH 7.4), and stored in storage buffer at a final concentration of 30 mg mL<sup>-1</sup>. The hairpin attached to the magnetic beads was annealed at 80 °C and slowly cooled to room temperature to allow formation of the hairpin structure. Then, the solution was kept at 4 °C in storage buffer for further use.

### **Etalon Fabrication**

The details of the paint-on technique used to fabricate microgel-based etalons for this study has been reported elsewhere.<sup>20</sup> In short, 25 × 25 mm pre-cleaned glass coverslips were rinsed with DI water and ethanol and dried with N<sub>2</sub> gas, and 2 nm of Cr followed by 15 nm of Au was thermally evaporated onto them at a rate of ~0.01 nm s<sup>-1</sup> and ~0.015 nm s<sup>-1</sup>, respectively,

using a thermal evaporation system by Torr International Inc. model THEUPG (New Windsor, NY). Here, Cr acts as an adhesion layer to hold the Au layer on the glass. The Au-coated substrates were annealed at 250 °C for 3 h followed by cooling to room temperature before use. The viscous microgel pellet purified previously contained in the centrifuge tube was vortexed to loosen the pellet and was placed on a hot plate at 30 °C. A previously coated Cr/Au substrate was rinsed with ethanol, dried with N<sub>2</sub>, and then placed onto the hot plate (Corning, NY) set to 30 °C. A 40 µL aliquot of the concentrated microgels was added to the substrate and then spread toward each edge using the side of a micropipette tip. The film was rotated 90°, and the microgel solution was spread again. The spreading and rotation continued until the microgels covered the entire substrate homogeneously and became too viscous to spread further. The microgels were allowed to dry completely on the substrate for 2 h with the hot plate temperature set to 35 °C. After 2 h, the dry film was rinsed copiously with DI water to remove any excess microgels not bound directly to the Au. Next, the film was placed into a DI water bath and allowed to incubate overnight on a hot plate set to 30 °C. Following this step, the substrate was again rinsed with DI water to further remove any microgels not bound directly to the Au substrate surface. Then, the film was dried with N<sub>2</sub> gas and placed into the thermal evaporator, and an additional 2 nm Cr followed by 15 nm Au was deposited onto the microgels as an overlayer. After the addition of the overlayer, the Au-microgel-Au structure (or etalon) was soaked in DI water overnight on a hot plate at 30 °C. The assemblies were then rinsed with DI water and dried with N<sub>2</sub> gas and subsequently used for experiments.

### **Reflectance Spectroscopy**

Reflectance spectra were collected with a USB2000+ spectrophotometer, an HL-2000-FHSA tungsten light source, and a R400-7-VIS-NIR optical fibre reflectance probe all from Ocean Optics (Dunedin, FL). The reflectance probe was always positioned normal to the etalon's surface. The spectra were recorded using Ocean Optics Spectra Suite Spectroscopy Software over a wavelength range of 350-1025 nm.

### **Experimental Setup for Biosensing**

The device was secured in a Petri dish using a piece of tape. Our previous studies showed that spatially isolated regions (e.g. small areas) of the etalon can behave in an independent fashion, and therefore solution can be added directly to the top of the etalon as a drop.<sup>22</sup> Before each experiment, different etalon sub-regions were soaked in 20  $\mu$ L DI water. Normally, the etalon was probed in four different sub-regions for the sensing. The light source was fixed with a clamp vertically over the liquid-exposed area of the device. The intensity and distance of light source from the assembly was adjusted to result in the highest quality reflectance spectra as determined by looking at the sharpness and intensity of the reflectance peaks. Before each measurement, we assured that the reflectance spectrum was stable, i.e., the position of the reflectance peaks was stable over time. Each experiment was repeated at least three times.

### **Protocol of Separating and Sensing RNA**

Specific volumes of target 2  $\mu$ M each of DNA and RNA (both with the same sequence, except that thymine in DNA was replaced by uracil in RNA) tagged with 6-carboxyfluorescein (FAM) and Cy5, respectively, were mixed into microcentrifuge tubes to yield molar ratios of 1:1 and 1:5 (RNA:DNA). An excess amount, relative to the RNA concentration, of MMPDNA (magnetic

microparticles with covalently attached ssDNA complementary to DNA) was added to the DNA/RNA solution mixtures, slowly stirred for 2 min and then kept for 24 h with occasional stirring at room temperature. After this time, an external magnet was placed on the outer wall of the microtube and held for 2 min. The magnet visibly pulled the magnetic microparticles towards the wall of the microcentrifuge tube. At this point, the unbound DNA should be suspended in the solution in the microcentrifuge tube, while the MMPDNA-RNA should be hybridized to the magnetic particle hairpins and stuck via the magnetic field to the wall of the centrifuge tube. The supernatant, presumably containing the unbound DNA, was pipetted out and the magnetic particles were washed several times with DI water. The supernatant and the washings were collected and their fluorescence spectra recorded. Next, 20  $\mu\text{L}$  of DI water was added to the separated and washed magnetic particle pellet and vortexed to resuspend them. Then, the magnetic particle solution was heated to 50 °C and then to 80 °C in a specific amount of DI water. Initially, the microcentrifuge tube was heated to 50 °C (well above the melting point of the DNA sequence used here and its complement) and kept at that temperature for 5 min. While the temperature was maintained, an external magnet was brought close to the outer wall of the microcentrifuge tube, held for 2 min, and the supernatant was pipetted out using a micropipette. At that temperature, due to the melting of DNA (if any) from the magnetic particles, all the DNA should be released into the supernatant solution while the RNA should remain hybridized to the attached hairpins on the magnetic microparticles. The supernatant was collected and an additional amount of DI water was added to the dry magnetic microparticle pellet. The above-mentioned procedure was repeated at 80 °C (well above the melting temperature of MMPDNA-RNA) and the supernatant, containing the RNA, was collected into a microcentrifuge

tube. The same procedure was repeated for the 1:5 RNA:DNA solution. The fluorescence and etalon measurements were made on the supernatants collected from both melts from the 1:1 and 1:5 mixtures of RNA:DNA solutions. A specific volume (20  $\mu\text{L}$ ) of the supernatant was added to the spot of the device, which was soaked with DI water and the optical properties were monitored as described above. We performed control experiments by repeating the same procedure with 10  $\mu\text{M}$  and 50  $\mu\text{M}$  DNA and 10  $\mu\text{M}$  RNA individually.

### **DNA/RNA Sequences Used in this Investigation:**

**Target DNA :** 5'-GTC GAG GTT AGG TTA CT-3'

**Target RNA :** 5'-GUC GAG GUU AGG UUA CU-3'

### **Probe Hairpin DNA :**

5'/5ThioMC6D/AAAAAAAAAAACCCAGTAACCTAACCTCGACACTGGG-3'

## **Results and Discussion**

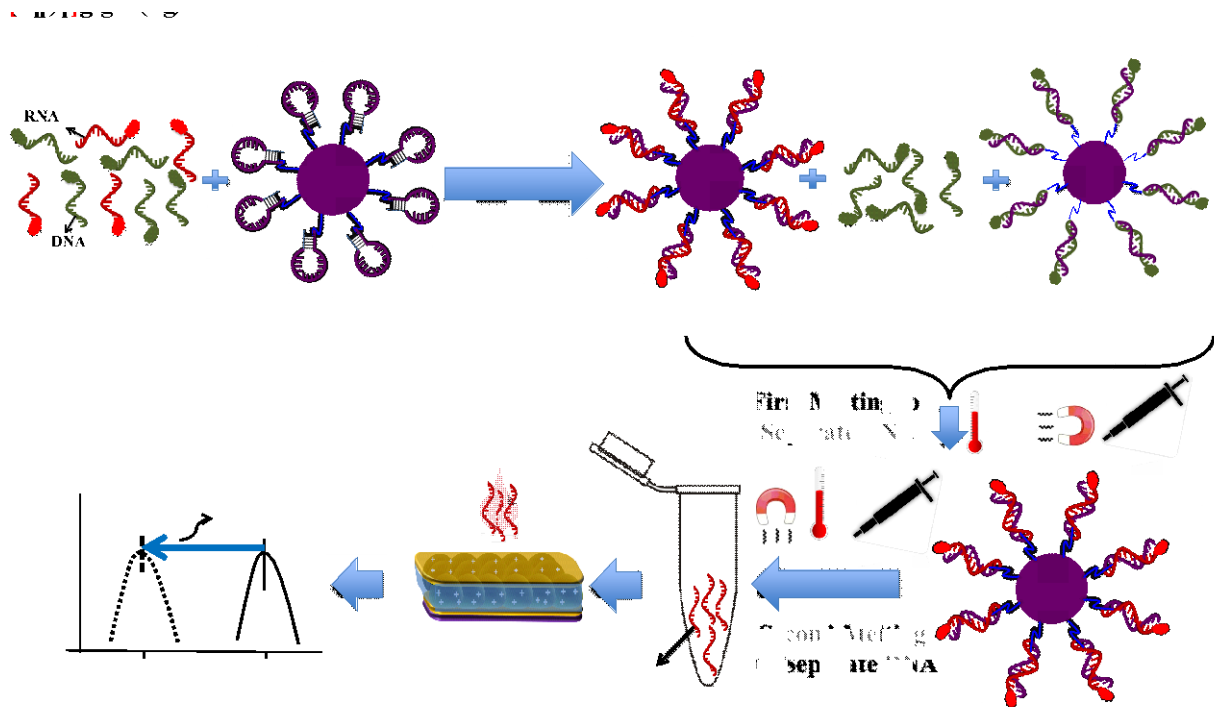
In our previous studies, we demonstrated that DNA of a specific sequence (target DNA) could be isolated from a solution using magnetic microparticles that were modified with DNA with the complementary sequence. The isolated DNA could then be added to an etalon composed of positively charged pNIPAm-co-APMAH microgels, which yielded a change in the position of the peaks ( $\lambda_{\text{max}}$ ) in the reflectance spectrum; the magnitude of the shift could then be related to the concentration of the DNA sequence in solution.<sup>23</sup> We attributed this to the negatively charged DNA entering the etalon's microgel layer, which could electrostatically crosslink the microgels

and cause them to collapse. The collapse ultimately led to a reduction in the distance between the etalons mirrors (d), which could be observed as a shift in the peaks in the etalon's reflectance spectrum. Here, we describe a method for separating a target RNA sequence from a mixture containing both RNA and DNA. This is a significant advance in the selectivity of the etalon-based sensor since both DNA and RNA are negatively charged. This method is based on the fact that the RNA-DNA hybrid duplex is stronger than the DNA-DNA duplex.

To accomplish the separation of RNA from DNA in the mixture, we functionalized magnetic microparticles with ssDNA (MMPDNA) designed to form a hairpin that is complementary to the target DNA or RNA. The hairpin was chosen because it shows greater discriminatory power and, hence, selectivity for the target RNA over the DNA compared to a straight ssDNA complement.<sup>24,25</sup> This greater selectivity arises because of the inherent balance in the hairpin between the stem hybridization and the loop hybridization with the target sequence. Any small disruption to this thermodynamic balance between the two hybridizations leads to a large equilibrium shift, leading to greater selectivity than a straight ssDNA complement may exhibit. This greater selectivity is achieved if the stem melting temperature ( $T_m$ ) is slightly ( $\sim 5$  °C) greater than the loop  $T_m$ .

The protocol used to separate the RNA from RNA-DNA mixture is depicted in Scheme 1. Once the MMPDNA was added to a mixture of the fluorescently labeled DNA and RNA, the Cy5-RNA should be selectively hybridized with the MMPDNA, forming the MMPDNA-RNA complex due to the stronger RNA-DNA hybrid duplex base-pairing while the FAM-DNA should stay suspended in the solution. The solution containing the FAM-DNA can be extracted by micropipette, while any hybridized or non-specifically bound DNA can be removed from the

magnetic microparticles by heating at 50 °C. Heating at 80 °C can then release any bound RNA. This combination of spatially separating the nucleic acids bound to the magnetic microparticles from the solution and differentially heating the mixture should be very effective at separating the weakly-bound DNA from the more strongly-bound RNA. Labelling the RNA and DNA with different fluorescent tags (FAM for the DNA and Cy5 for the RNA) allows the separation to be measured and quantified.



Scheme 1: A schematic illustrating the separation of RNA from a mixture containing DNA via MMPDNA-mediated isolation, differential melting, and subsequent sensing via exposure of the isolated RNA to an etalon. The mixture of DNA and RNA was added to MMPDNA and incubated with occasional stirring at room temperature. The mixture was heated to 50 °C and the

solution was extracted while keeping an external magnet close to the wall of the micro-centrifuge tube. This step removes the unbound and bound DNA from the mixture leaving behind MMPDNA-RNA. The MMPDNA-RNA solution was heated to 80 °C to allow the RNA to melt off the MMPDNA into the solution. While the solution was kept at 80 °C, an external magnet was brought close to the wall of the microcentrifuge tube and the RNA-containing solution was removed. The extracted solution was added to the etalon and the optical response recorded.

Fig. 2 shows a plot of shift in  $\lambda_{\max}$  with the addition of supernatant collected at 80 °C from RNA:DNA (1:1) and RNA:DNA (1:5). These extracts should only contain RNA. We observed a shift of approximately 13 nm when we added supernatant extracted from RNA:DNA (1:1). This shift confirms that the magnetic beads were able to bind the RNA from the RNA:DNA solution. Even if the magnetic beads bind some DNA, those would be selectively removed due to the differential melting temperatures (see below). We want to mention here that we observed similar shift in magnitude with addition of ssDNA only in a separate control experiment. The shift is related to the negatively charged phosphate groups present both in DNA and RNA. To show that the separation of RNA and DNA was occurring with this differential melting, we performed a control experiment where only a DNA solution was used following the same protocol. After the separation of magnetic beads, subsequent differential melting and washing, we added the supernatant solution to the pNIPAm-co-APMAH etalons and did not observe any noticeable

change in the position of the reflectance peak. On the other hand, when we added the 80 °C extract from the RNA: DNA (1:5) solution, we observed only a negligible shift in  $\lambda_{\max}$ , comparable to what was observed from the DNA-only control shift suggesting that only a small amount of Cy5-RNA and/or DNA is bound to the MMPDNA. We hypothesize that Cy5-RNA was unable to compete with the very high concentration of FAM-DNA resulting in mostly the FAM-DNA/MMPDNA duplex being formed. As a result, after the differential melting there was no RNA bound onto the MMPDNA to be extracted, so we did not notice any change in the position of the peaks in the reflectance spectra from the etalon. We further tested this hypothesis by performing a fluorescence experiment on the different extracts.

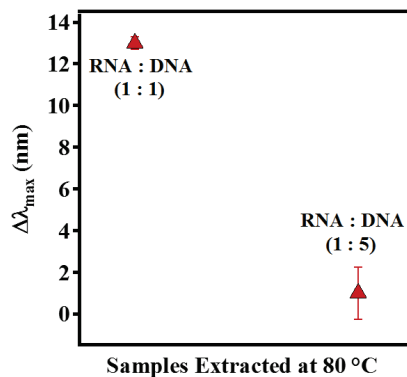


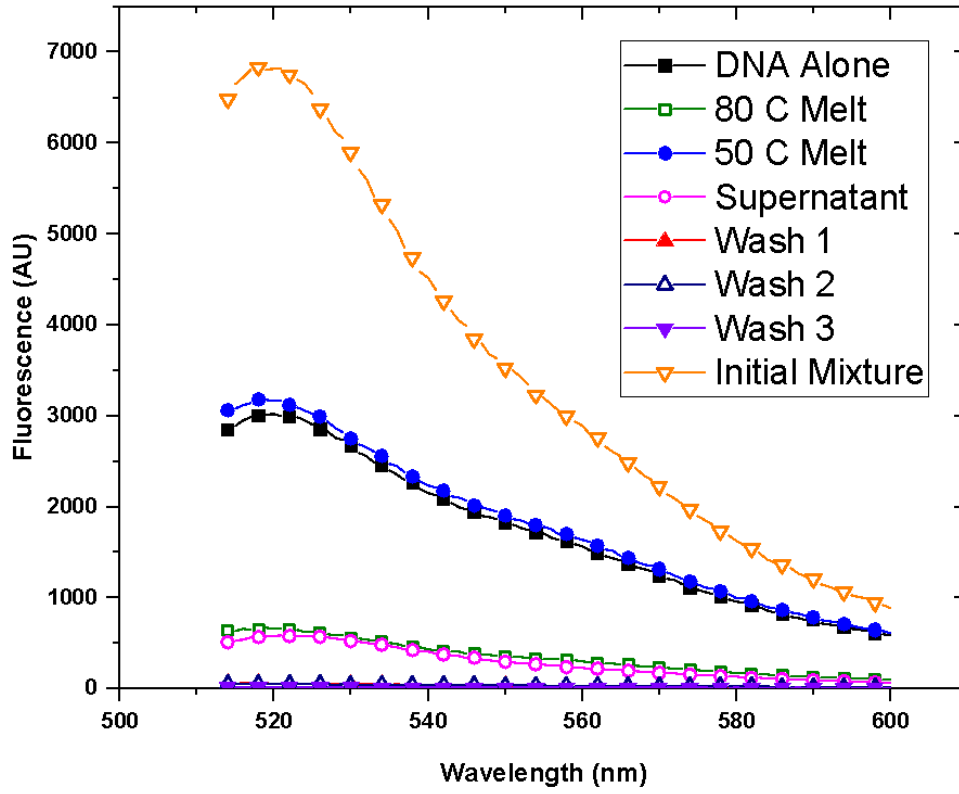
Fig. 2: The shift of the  $\lambda_{\max}$  on addition of RNA extracts from a mixture of DNA and RNA by differential melting. Similar shifts were seen for the 50 °C extracts. A DNA-only solution, following the same protocol, yielded only a 2-3 nm shift, similar to what is seen for the 1:5 RNA:DNA mixture.

To justify the above observations and confirm the separation of RNA we studied the fluorescence spectra of the extracts collected at different separation and washing steps detailed above. Fig. 3 shows the fluorescence studies of the extracts collected from the different stages of separation of Cy5-RNA from FAM-DNA for the 1:1 solution, and Fig. 4 shows the same for the 1:5 solution. The fluorescence emission spectra were collected by excitation at 520 nm for FAM-DNA and 670 nm for Cy5-RNA. We concluded that we were able to separate the Cy5-RNA from FAM-DNA by MMPDNA as shown in Fig. 3. Fig. 3a shows that the first melting was necessary to eliminate the presence of DNA from the mixture, and that the FAM fluorescence signal from this extract matches the FAM fluorescence signal from the 2  $\mu$ M DNA initially used in the solution. Thus, the MMPs bind DNA and RNA equally well at room temperature. However, the DNA is less stabilized in the hybrid compared to RNA, and the DNA thus melts completely off the MMPs at a lower temperature,  $\leq 50$   $^{\circ}$ C. That the FAM fluorescence signal in the 80  $^{\circ}$ C extract is the same as baseline indicates that all the DNA was melted off the MMPs in the 50  $^{\circ}$ C melt step and no FAM signal is seen in subsequent washes 1-3.

Fig. 3b shows the Cy5 channel, which monitors the RNA concentration and can track the presence of RNA in the different solutions through the protocol. As expected, the initial mixture shows the same signal in this channel as the initial 2  $\mu$ M RNA solution alone. The extract from the 50  $^{\circ}$ C melt shows no detectable Cy5 fluorescence signal, verifying that this temperature is insufficient to melt the RNA off the MMP. Upon melting at 80  $^{\circ}$ C, the FAM signal increases, indicating melting of the RNA off the MMP as expected, but a surprising result is that the FAM signal increases above the original signal by roughly a factor of 2. Similar fluorescence

quenching of Cy5 has been seen with gold nanoparticles.<sup>26</sup> Subsequent washes again show no evidence of RNA, indicating that melting of both DNA and RNA is complete at 50 °C and 80 °C, respectively. It is important to note that we observed a reproducible strong enhancement of the fluorescent emission of FAM-DNA in the presence of Cy5-RNA, as shown by the *stronger* FAM signal for the initial 1:1 mixture than for the 2 mM DNA alone, at equivalent FAM concentrations, in Fig. 3a. This strong and rather unusual enhancement is currently under further investigation.

**A**



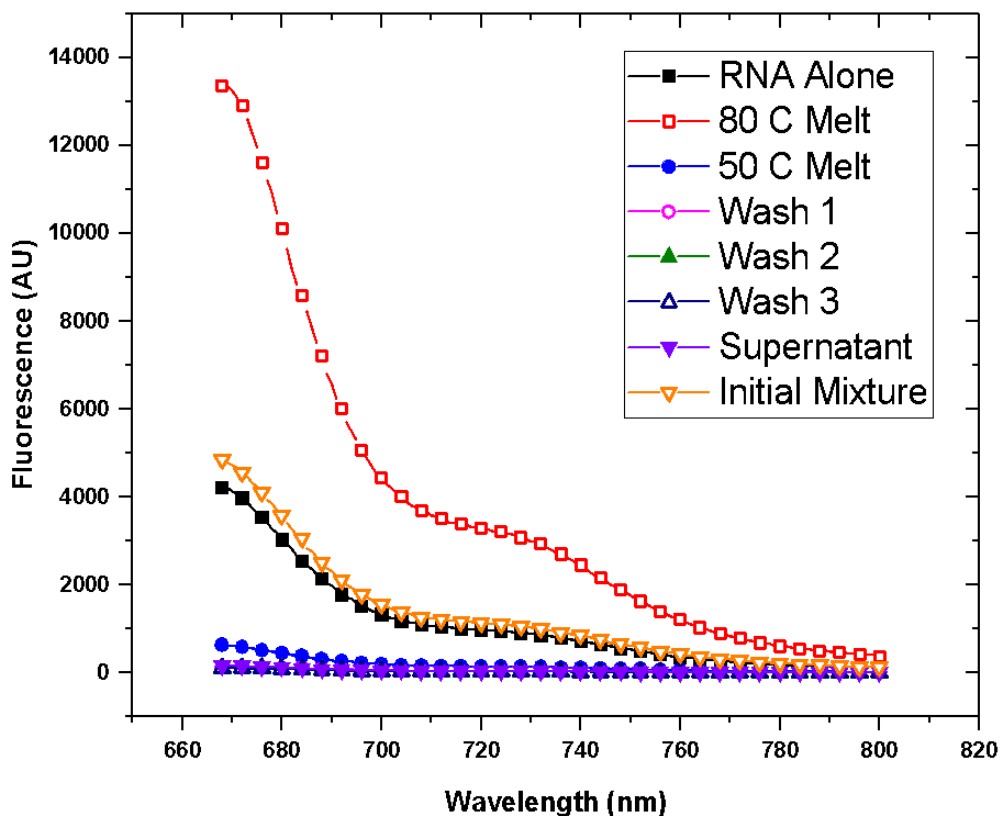
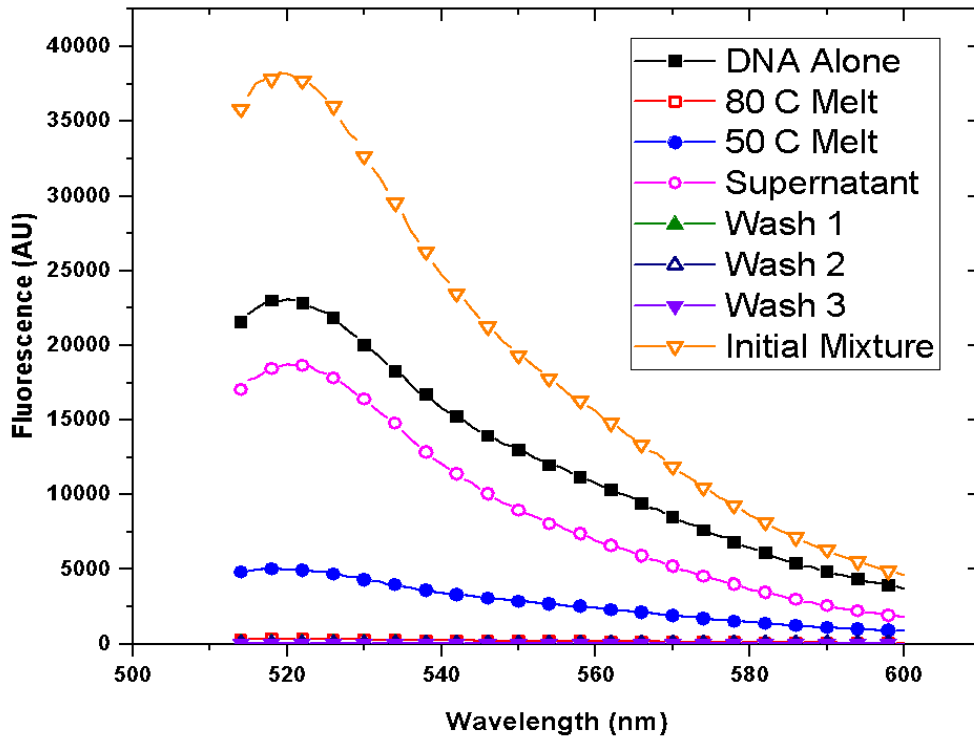
**B**

Fig. 3: The fluorescence spectra of the 1:1 Cy5-RNA:FAM-DNA at various stages in the separation and detection process excited at (a) 520 nm (FAM channel) and (b) 670 nm (Cy5 channel). Here, "Supernatant" means the remaining liquid after magnetic separation of the MMPDNA beads by external magnet, and "Wash 1", "Wash 2" and "Wash 3" are the solutions collected as washings with DI water after magnetic separation of the magnetic microparticle beads and subsequent collection of the remaining solutions derived from the mixture. Magnetic separation was done at 50 °C and 80 °C while the remaining solutions were collected by melting

the DNA-DNA and DNA-RNA duplex, which are labelled as "50 °C Melt" and "80 °C Melt", respectively.

We also observed that we were able to separate the Cy5-RNA from FAM-DNA by MMPDNA for the 1:5 solution, but with much less discrimination, as shown in Fig. 4. Here, the FAM signal indicates the presence or absence of DNA in the various extracts throughout the process, and its concentration. The FAM signal from the supernatant after hybridization is almost the same as the DNA alone, indicating that little of the DNA hybridized. That is not surprising, since the DNA is in excess compared to the concentration of binding sites on the MMP. After melting at 50 °C, all the DNA again melts off as for the 1:1 solution. No FAM signal is observed for the 80 °C melt or for the subsequent washes. A similar behavior for the 1:5 solution is observed as for the 1:1 solution in the Cy5 channel; the initial Cy5 signal of the 1:5 solution is the same as for the RNA alone and all the RNA shows up in the extract only after melting to 80 °C. Again, the rather surprising enhancement of FAM fluorescence in the FAM-DNA: Cy5-RNA solution is observed in Fig. 4a, where the FAM fluorescence intensity from the RNA:DNA solution is *higher* than for the DNA solution alone at equivalent concentrations of FAM. Fig. 4b shows the competition of the excess DNA with RNA and the effectiveness of the separation method by MMPDNA and differential melting. A very negligible shift in the Cy5 channel for RNA confirms that only an insignificant amount of RNA can be present after second melting.

A



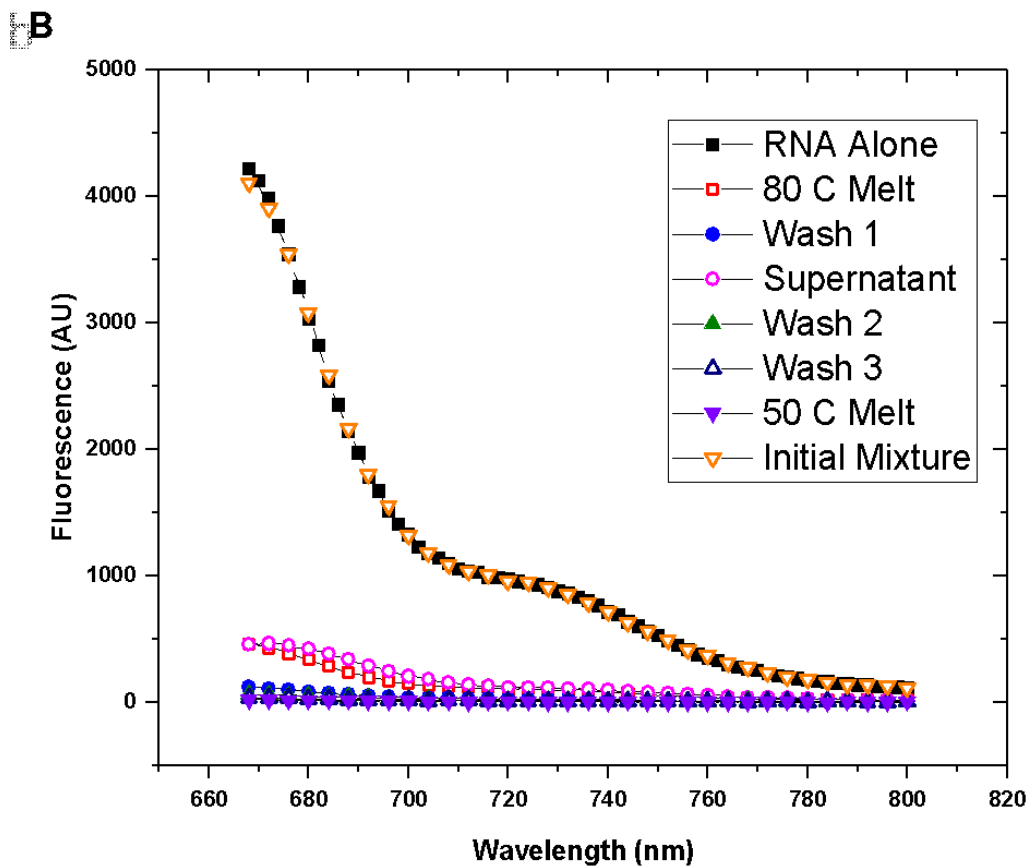


Fig. 4: The fluorescence spectra of the 1:5 Cy5-RNA:FAM-DNA at various stages in the separation and detection process excited at (a) 520 nm (FAM channel) and (b) 670 nm (Cy5 channel). Here, "Supernatant" means the remaining liquid after magnetic separation of the MMPDNA beads by external magnet, and "Wash 1", "Wash 2" and "Wash 3" are the solutions collected as washings with DI water after magnetic separation of the magnetic microparticle beads and subsequent collection of the remaining solutions derived from the mixture. Magnetic

separation was done at 50 °C and 80 °C while the remaining solutions were collected by melting the DNA-DNA and DNA-RNA duplex which are labelled as "50 °C Melt" and "80 °C Melt", respectively.

## **Conclusion**

In summary, we have shown that RNA can be selectively separated from a RNA:DNA mixture by utilizing hairpin functionalized magnetic beads and sensed by an etalon. Here, we found that the thermoresponsive pNIPAm-*co*-APMAH microgel-based etalon can be used to detect the presence of RNA. The porous Au overlayer allows the negatively charged RNA to penetrate into the microgel layer, causing them to collapse, leading to a shift in the peaks in the reflectance spectra. Fluorescence studies confirmed the separation of RNA from DNA. We believe that this colorimetric approach of separation will help us build low cost point-of-care devices for the resources limited areas of the world.

## **Acknowledgements**

MJS acknowledges funding from the University of Alberta (the Department of Chemistry and the Faculty of Science), the Natural Sciences and Engineering Research Council of Canada

(NSERC), the Canada Foundation for Innovation (CFI), the Alberta Advanced Education & Technology Small Equipment Grants Program (AET/SEGP), IC-IMPACTS and Grand Challenges Canada. MJS and GRL acknowledge Mark McDermott for the use of the thermal evaporator and Robert Campbell for the use of fluorescence spectrometer. GRL acknowledges funding from the Natural Sciences and Engineering Research Council of Canada (NSERC) and the Alberta Heritage Foundation for Medical Research (AHFMR).

## References

- (1) Ahrberg, C. D.; Manz, A.; Neuzil, P. *Anal. Chem.* **2016**, *88*, 4803.
- (2) Rio, D. C.; Ares, M. Jr.; Hannon, G. J.; Nilsen, T. W. *RNA: A Laboratory Manual*. Cold Spring Harbor: Cold Spring Harbor Laboratory Press, Cold Spring Harbor, NY **2011**, pp 586.
- (3) Osborne, R. J.; Thornton, C. A. *Hum. Mol. Genet.* **2006**, *15*, R162.
- (4) Angaji, S.A.; Hedayati, S.S.; Poor, R.H.; Madani, S.; Poor, S.S.; Panahi, S. *J. Genet.* **2010**, *89*, 527.
- (5) Marsella, M. J.; Carroll, P. J.; Swager, T. M. *J. Am. Chem. Soc.* **1995**, *117*, 9832.
- (6) Kim, J.; Nayak, S.; Lyon, L. A. *J. Am. Chem. Soc.* **2005**, *127*, 9588.
- (7) Pelton, R. *Adv. Colloid Interface Sci.* **2000**, *85*, 1.
- (8) Saunders, B. R., Lyon, L. A. (ed.) & Serpe, M. J. (ed.) 2012 *Hydrogel, micro and nanoparticles*. Weinheim: Wiley - VCH Verlag GmbH & CO. KGaA, p. 141-168.

- (9) Stuart, M. A. C.; Huck, W. T. S.; Genzer, J.; Muller, M.; Ober, C.; Stamm, M.; Sukhorukov, G. B.; Szleifer, I.; Tsukruk, V. V.; Urban, M.; Winnik, F.; Zauscher, S.; Luzinov, I.; Minko, S. *Nat. Mater.* **2010**, *9*, 101.
- (10) Wu, C.; Wang, X. *Phys. Rev. Lett.* **1998**, *80*, 4092.
- (11) Wu, C.; Zhou, S. Q. *Macromolecules* **1995**, *28*, 5388.
- (12) Hoare, T.; Pelton, R. *Macromolecules* **2004**, *37*, 2544.
- (13) Kanazawa, H.; Yamamoto, K.; Matsushima, Y.; Takai, N.; Kikuchi, A.; Sakurai, Y.; Okano, T. *Anal. Chem.* **1996**, *68*, 100.
- (14) Hoare, T.; Pelton, R. *Biomacromolecules* **2008**, *9*, 733.
- (15) Kim, D.-H.; Vitol, E. A.; Liu, J.; Balasubramanian, S.; Gosztola, D. J.; Cohen, E. E.; Novosad, V.; Rozhkova, E. A. *Langmuir* **2013**, *29*, 7425.
- (16) Zhang, Q. M.; Xu, W.; Serpe, M. J. *Angew. Chem., Int. Ed.* **2014**, *53*, 4827.
- (17) Islam, M. R.; Serpe, M. J. *Chem. Commun.* **2013**, *49*, 2646.
- (18) Islam, M. R.; Serpe, M. J. *Anal. Bioanal. Chem.* **2014**, *406*, 4777.
- (19) Gao, Y.; Zago, G. P.; Jia, Z.; Serpe, M. J. *ACS Appl. Mater. Interfaces* **2013**, *5*, 9803.
- (20) Islam, M. R.; Serpe, M. J. *Macromolecules* **2013**, *46*, 1599.
- (21) Hill, H. D.; Mirkin, C. A. *Nat. Protoc.* **2006**, *1*, 324.
- (22) Sorrell, C. D.; Carter, M. C. D.; Serpe, M. J. *ACS Appl. Mater. Interfaces* **2011**, *3*, 1140.
- (23) Hu, L.; Serpe, M. J. *J. Mater. Chem.* **2012**, *22*, 8199.

- (24) Bonnet, G.; Tyagi, S.; Libchaber, A.; Kramer, F. R. *Proc. Natl. Acad. Sci. USA* **1999**, *96*, 6171.
- (25) El-Yazbi, A. F.; Loppnow, G. R. *Tr. Anal. Chem.* **2014**, *61*, 83.
- (26) Acuna, G. P.; Bucher, M.; Stein, I. H.; Steinhauer, C.; Kuzyk, A.; Holzmeister, P.; Schreiber, R.; Moroz, A.; Stefani, F. D.; Liedl, T.; Simmel, F. C.; Tinnefeld, P. *ACS Nano* **2012**, *6*, 3189.